Droplet relaxation in blends with one viscoelastic component: Bulk and confined conditions

R. Cardinaels and P. Moldenaers

Lab for Applied Rheology and Polymer Processing

Department of Chemical Engineering

KU Leuven

Willem de Croylaan 46, Box 2423, B-3001 Leuven, Belgium

Paula.Moldenaers@cit.kuleuven.be

Final accepted draft

Cite as: R. Cardinaels, P. Moldenaers, Rheol. Acta, 49(9), pp. 941-951 (2010)

The original publication is available at www.springerlink.com.

http://link.springer.com/article/10.1007%2Fs00397-010-0460-y

Rheologica Acta manuscript No.
(will be inserted by the editor)

Droplet relaxation in blends with one viscoelastic component: Bulk and confined conditions

Cardinaels Ruth · **Moldenaers Paula**

Received: date / Accepted: date

Abstract Using a counter rotating parallel plate shear flow cell, the shape relaxation of deformed droplets in a quiescent matrix is studied microscopically. Both the effects of geometrical confinement and component viscoelasticity are systematically explored at viscosity ratios of 0.45 and 1.5. The flow conditions are varied from a rather low to a nearly critical Ca-number. Under all conditions investigated, viscoelasticity of the droplet phase has no influence on shape relaxation, whereas matrix viscoelasticity and geometrical confinement result in a slower droplet retraction. Up to high confinement ratios, the relaxation curves for ellipsoidal droplets can be superposed onto a master curve. Confined droplets with a sigmoidal shape relax in two stages; the first consists of a shape change to an ellipsoid with a limited amount of retraction, the second is the retraction of this ellipsoid. The latter can be

R. Cardinaels · P. Moldenaers

Department of Chemical Engineering,

Katholieke Universiteit Leuven,Willem de Croylaan 46,

B-3001 Leuven, Belgium

Tel.: +3216322359

Fax.: +3216322991

E-mail: paula.moldenaers@cit.kuleuven.be

described by means of one single relaxation time, that can be obtained from the relaxation of initially ellipsoidal droplets. The experimental results are compared to the predictions of a recently published phenomenological model for droplet dynamics in confined systems with viscoelastic components (Minale et al. 2010). However, whereas the model predicts additive effects of geometrical confinement and component viscoelasticity, the experimental data reveal more complex interactions.

Keywords Single droplet dynamics · Shape relaxation · Viscoelasticity · Confinement · Minale model

1 Introduction

Since the pioneering work of Taylor (1932, 1934), droplet dynamics in blends and emulsions has been studied extensively (as reviewed by Rallison (1984), Stone (1994), Briscoe (1999), Tucker and Moldenaers (2002), Guido and Greco (2004),Van Puyvelde and Moldenaers (2005) and Van Puyvelde et al. (2008)). In single droplet studies the focus is often on droplet deformation and breakup. However, for blends of molten polymers, the final morphology after processing will also depend on the details and kinetics of the shape relaxation. Several parameters such as cooling speed, fluid rheology and interactions with other droplets or the walls of the processing equipment can influence this relaxation process and consequently the droplet shape and size in the final product. It can also be noted that shape relaxation of deformed droplets has become a popular way to determine the interfacial tension of a blend (Guido and Greco 2004).

Although they are often used as a model system, emulsions and blends consisting of Newtonian components have limited practical applications. Mostly, the blend constituents are viscoelastic rather than Newtonian. The blend morphology often needs to be stabilized against coarsening by means of compatibilizers or colloidal particles (as reviewed by Van Puyvelde and Moldenaers (2005) and Fenouillot et al. (2009)). In addition, the processing equipment commonly consists of sophisticated devices in which the material is subjected to complex flow fields. Finally, microfluidics and microscale polymer processing are gaining importance, which implies that the influence of the walls can not be neglected. All these complications should be included in design and optimization calculations of processing operations. Obviously, from a research point of view, this problem cannot be tackled in its complexity at once. Therefore, research focusses on model type problems that deal with certain of these

aspects in order to gather fundamental insight in morphology development.

For blends consisting of Newtonian components, the droplet deformation in shear flow depends on the capillary number Ca (= $\eta_m \cdot \dot{\gamma} \cdot$ R / Γ, where η_m, $\dot{\gamma}$, R and Γ denote respectively matrix viscosity, shear rate, droplet radius and interfacial tension) and the viscosity ratio λ (= η_d / η_m, with η_d the droplet viscosity). The droplet deformation increases with increasing Ca and when Ca exceeds a critical value Ca_{crit}, the droplet will deform irreversibly under flow until eventually breakup occurs. The Ca_{crit} as a function of λ has carefully been mapped out by Grace (1982). The relaxation of such droplets after cessation of a subcritical shear flow is well-documented and can be reproduced by model predictions (Guido and Villone 1999; Mo et al. 2000; Guido and Greco 2001). For ellipsoidal droplets, the shape relaxation process can be described by means of one single relaxation time (Luciani et al. 1997; Guido and Villone 1999; Mo et al. 2000). It was observed both experimentally (Vananroye et al. 2008) and numerically (Janssen and Anderson 2007) that confinement of the droplets (e.g. between two parallel plates) retards the retraction process. Vananroye et al. (2008) have shown that in systems with Newtonian components, the shape relaxation of a confined droplet is well described by the confined Minale model (Minale 2008). The latter is a phenomenological model that describes the dynamics of ellipsoidal droplets for systems with Newtonian components in a generic confined flow.

In order to gain insight into the droplet dynamics of systems with industrial relevance, the effect of viscoelasticity of the components needs to be considered. This topic received quite some attention during the last decade (Guido and Greco 2004; Van Puyvelde and Moldenaers 2005). When the matrix is viscoelastic, droplet retraction is considerably retarded as compared to the Newtonian case (Maffettone and Greco 2004; Yu et al. 2004; Yu et al.

2005; Yue et al. 2005; Sibillo et al. 2006; Verhulst et al. 2007, 2009b). For blends with a viscoelastic Boger fluid matrix, the deformation of ellipsoidal droplets does not decrease exponentially, as in systems with Newtonian components, but the retraction is retarded at the later stages, leading to a tail in the shape relaxation curves (Sibillo et al. 2006; Verhulst et al. 2007, 2009b). This tail can only be modeled by using constitutive equations for the viscoelastic fluid that have at least two relaxation times (Yu et al. 2004; Yu et al. 2005; Yue et al. 2005; Verhulst et al. 2009a). Droplet viscoelasticity has been shown to have less influence on the shape relaxation of deformed droplets (Lerdwijitjarud et al. 2003; Verhulst et al. 2009b).

In this work, we specifically study the combined effect of geometrical confinement and component viscoelasticity on the shape relaxation of deformed droplets with varying degrees of initial deformation. To our knowledge, no such systematic study has been reported on yet, except for some preliminary results reported by the present authors (Cardinaels et al. 2007, 2008). Results on the combined effect of confinement and viscoelasticity of one of the components on the steady state droplet behaviour have recently been published elsewhere (Cardinaels et al. 2009). As transient experiments are critical for model assessment, it will be verified in the present work to which extent a very recently published phenomenological model that can describe the combined effects of confinement and component viscoelasticity on the dynamics of ellipsoidal droplets (Minale et al. 2010), can be used to describe shape relaxation after cessation of shear flow. For these conditions, the model has only been validated to a very limited extent for the case of a viscoelastic matrix.

2 Materials and methods

Droplet retraction after cessation of shear flow is visualized in a flow cell that consists of two transparent parallel plates that can rotate in opposite directions. The device is a modification of a Paar Physica MCR300 rheometer. With the setup, a droplet in a stagnation plane can be studied microscopically from both the vorticity and the velocity gradient direction. The operating principle and details of the experimental setup have been presented elsewhere (Verhulst et al. 2007; Cardinaels et al. 2009).

The polymers and blends used in this study are summarized in Table 1, where d denotes droplet and m matrix. Blends with either a viscoelastic matrix or a viscoelastic droplet were used in order to study the effects of component viscoelasticity on the shape relaxation. As viscoelastic material, a polyisobutylene (PIB) Boger fluid (BF2, see Verhulst et al. (2007, 2009a,b)), containing 0.2 w% of a high molecular weight polymer ($M_v = 4.10^6$) was used. This viscoelastic material was combined with mixtures of polydimethylsiloxane (PDMS) with different viscosities to obtain blends with viscosity ratios of 0.45 and 1.5. The bulk critical Ca-numbers Ca_{crit} associated with these viscosity ratios are 0.46 and 0.56 respectively for purely Newtonian components (De bruijn 1989). Under the studied conditions, component viscoelasticity does not substantially influence the Ca_{crit} in bulk shear flow (Cardinaels et al. 2008). In the shear rate range of interest, all PDMS samples are Newtonian whereas the fluid BF2 is viscoelastic and has a viscosity and first normal stress coefficient that are independent of shear rate. At the experimental temperatures, the polymer relaxation time τ_p of the BF2 fluid, as calculated from the Oldroyd-B model ($\tau_p = \Psi_1/\eta_p$, where Ψ_1 and η_p denote respectively the first normal stress coefficient and the polymer contribution to the viscosity), is approximately 8.5 s (Verhulst et al. 2009a). Although the Oldroyd-B

model is frequently used to describe the rheology of Boger fluids, these fluids in principle have a spectrum of relaxation times (Quinzani et al. 1990). Verhulst et al. (2009a) reported that the steady rheology of BF2 can be well-described by a 5-mode Giesekus model with a longest relaxation time of 49 s. The interfacial tension of the blends was determined by fitting the slow flow droplet deformation data to the second order theory of Greco (Greco 2002).

Table 1 Blend and component characteristics

Blend	d/m	Droplet	Matrix	T	η_m	$\Psi_{1,d}$	$\Psi_{1,m}$	Γ	λ
				°C	Pa.s	Pa.s^2	Pa.s^2	mN/m	-
1	N/VE	PDMS30-100	BF2	26.4	36.5	0	197	2.0	1.5
2	VE/N	BF2	PDMS30	26.0	25.2	212	0	2.2	1.5
3	N/VE	PDMS12,5-30	BF2	26.2	37.2	0	204.5	2.0	0.45
4	VE/N	BF2	PDMS100	26.2	82.6	204.5	0	1.85	0.45

3 Phenomenological models including confinement and component viscoelasticity

The experimental results are compared with the predictions of phenomenological models for the dynamics of ellipsoidal droplets. In unbounded flow and for systems with Newtonian components, the three droplet axes L, B and W and the droplet orientation with respect to the flow direction are well described by the Maffettone-Minale model (Maffettone and Minale 1998). In this model, the droplet shape is represented by a symmetric, positive-definite, second rank tensor **S**, with eigenvalues representing the squared dimensionless semiaxes of

the ellipsoid. The dynamics of **S** are dictated by the following equation:

$$\frac{\mathrm{d}\mathbf{S}}{\mathrm{d}t} - Ca\left(\Omega\cdot\mathbf{S}-\mathbf{S}\cdot\Omega\right) = -f_1\left[\mathbf{S}-g(\mathbf{S})I\right] + Ca\cdot f_2\left(\mathbf{D}\cdot\mathbf{S}+\mathbf{S}\cdot\mathbf{D}\right) \quad (1)$$

where t is the time that is made dimensionless with the emulsion time τ_{em} = $(\eta_m \cdot R/\Gamma)$, **D** is the dimensionless deformation rate tensor and Ω the dimensionless vorticity tensor. The function $g(\mathbf{S})$ is introduced to preserve the droplet volume, while f_1 and f_2 are non-dimensional, non-negative functions of Ca and λ that are derived to make the model recover the small-deformation theory of Taylor (1934) at low Ca.

For nearly spherical droplets, the effects of geometrical confinement on the steady droplet deformation have been calculated theoretically by Shapira and Haber (1990). It was found that the droplet deformation increases with the ratio of droplet diameter 2R to gap spacing H to the power 3. In order to extend the results of this small-deformation theory to higher deformations or to transient flow conditions, the original Maffettone-Minale model has been adapted for confined flows. Vananroye et al. (2007) proposed an expression for the steady state droplet deformation parameter that consists of a combination of the bulk deformation parameter from the Maffettone-Minale model with an additional wall factor obtained from the Shapira-Haber theory. Recently, a modified version of the Maffettone-Minale model was developed that enables the prediction of the transient droplet behaviour under confined conditions (Minale 2008). If the blend components are Newtonian, Eq. 1 remains valid. To include the effects of confinement, the expressions for f_1 and f_2 were extended to take into account the dependence on the ratio of droplet radius R to gap height H.

Effects of component viscoelasticity on the steady droplet deformation only appear at the

second order in Ca (Greco 2002). Therefore, adapted evolution equations for **S** have been proposed to include effects of viscoelasticity of the components (Maffettone and Greco 2004; Minale 2004). For example, in the evolution equation formulated by Minale, the following term is added to the right-hand side of Eq. 1:

$$Ca \cdot f_3 \Big[\big(\mathbf{D}\cdot\mathbf{S}\cdot\mathbf{S}+\mathbf{S}\cdot\mathbf{S}\cdot\mathbf{D}\big) - \big(\mathbf{D}\cdot\mathbf{S}+\mathbf{S}\cdot\mathbf{D}\big)\frac{1}{3}\big(\mathbf{S}:\mathbf{I}\big) \Big] \tag{2}$$

In this case, the parameters f_1, f_2 and f_3 also depend on the Deborah number De (= $\Psi_1 \cdot \Gamma/(2R\cdot\eta^2)$) and the ratio Ψ of the second to the first normal stress difference for each component.

In order to include the effects of confinement on the steady state droplet deformation for blends with viscoelastic components, Cardinaels et al. (2009) combined the expression for the bulk deformation parameter for systems with viscoelastic components with the Newtonian Shapira-Haber factor for wall effects. Very recently, the phenomenological Minale model (Minale 2004) for droplet dynamics in bulk systems with viscoelastic components has been extended to confined flows (Minale et al. 2010). To that end, the dependence of the functions f_1 and f_2 on the ratio R/H was taken similar as in the confined Minale model for systems with Newtonian components (Minale 2008). In addition, f_3 was chosen to depend on the ratio R/H to the power 3. In the present work, the phenomenological models for confined droplet dynamics in systems with Newtonian (Minale 2008) or viscoelastic components (Minale et al. 2010) will be validated for shape relaxation after cessation of shear flow.

4 Results and discussion

Since droplet deformation and therefore also droplet retraction is the most pronounced for the droplet longest axis L, measurements of this axis provide accurate information about the shape relaxation. However, with our experimental setup, determination of the droplet dimensions in the velocity - vorticity plane is far less complicated than in the velocity - velocity gradient plane (Verhulst et al. 2007). Therefore, most of the time the projection L_p of the longest droplet axis L in the velocity direction is used to quantitatively describe the shape relaxation. It was checked that the orientation angle during relaxation remains constant, even for confined droplets. In all figures, time is scaled with the emulsion time $\tau_{em} = \eta_m \cdot R/\Gamma$ and the droplet axis L_p is scaled between 0 and 1. The subscript 0 denotes the start of the shape relaxation process. Unless stated otherwise, the droplet size is chosen in such a way that the Deborah number has a fixed value of 1.

4.1 Shape relaxation after shear flow at a low Ca

In this section, the shape relaxation of droplets after cessation of shear flow with a rather low Ca (= 0.2), as compared to the critical value, will be discussed. The evolution of the dimensionless droplet axes of a viscoelastic droplet with λ = 1.5 in a Newtonian matrix (Blend 2 in Table 1) are shown in Fig. 1 for an unbounded droplet and a droplet with 2R/H = 0.74. The predictions of the confined Minale models for systems with Newtonian (Minale 2008) and viscoelastic components (Minale et al. 2010) are also added. As initial droplet dimensions for the model predictions, the experimental dimensionless droplet axes have been used. In addition, for blends with viscoelastic components, the parameter Ψ has been fixed at 0.1 throughout this work, in agreement with earlier studies (Verhulst et al. 2007; Cardinaels et al. 2009; Minale et al. 2010). It can be seen that geometrical confinement increases the

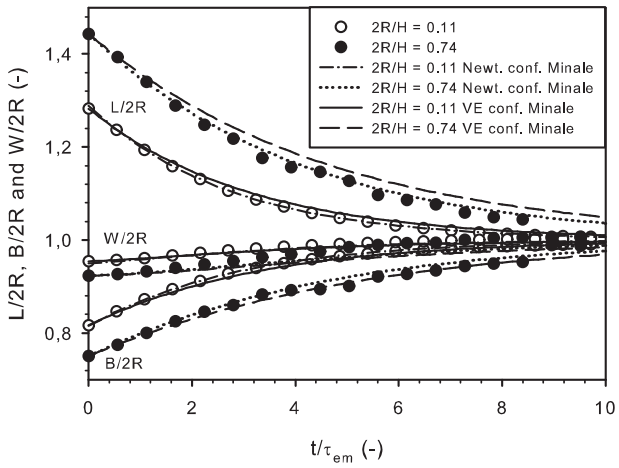

Fig. 1 Dimensionless droplet axes during shape relaxation after cessation of shear flow with Ca = 0.2; Viscoelastic droplet in a Newtonian matrix with λ = 1.5, experimental data (symbols) and predictions of the confined Minale models (Minale 2008; Minale et al. 2010) (lines)

initial droplet length and retards the retraction of all three droplet axes, as in earlier work (Vananroye et al. 2007, 2008; Cardinaels et al. 2009). The experimental data coincide with the predictions of the confined Minale model for systems with Newtonian components. However, the model predicts a somewhat slower relaxation when the droplet is viscoelastic, a trend that is not observed in the experimental data.

In Fig. 2 results for the retraction of the longest droplet axis of a viscoelastic droplet in a Newtonian matrix (same blend as in Fig. 1) are shown for a series of degrees of confinement, defined as 2R/H. From these data it is clear that the relaxation is slowed down if the confinement ratio 2R/H exceeds 0.5. In addition, by using a graph with a semi-logarithmic scale, straight lines are obtained for the retraction curves, which implies that the shape relaxation process can be described by means of one single relaxation time τ, even for confined

droplets. Exponential relaxation curves with an increasing relaxation time for increasing degrees of confinement were also obtained for systems that contain only Newtonian components (Vananroye et al. 2008). In addition, Vananroye et al. (2008) showed that the confined Minale model provides good agreement with the experimental results for droplet relaxation in these blends. The predictions of the confined Minale model (Minale 2008) for systems with Newtonian components are added to Fig. 2. The agreement between the experimental data and the model predictions is excellent, even up to the highest confinement ratio. Therefore, the conclusion of Verhulst et al. (2009b) that, at a viscosity ratio of 1.5, droplet viscoelasticity does not influence droplet relaxation in bulk conditions, can be extended to highly confined conditions. However, the confined Minale model for systems with viscoelastic components (Minale et al. 2010) clearly overpredicts the relaxation time at 2R/H = 0.74.

Relaxation after cessation of shear flow with Ca = 0.2 is also studied here for a system with a viscoelastic matrix at λ = 1.5 (Blend 1 in Table 1). The evolution of the three dimensionless droplet axes is presented in Fig. 3 for an unbounded and a confined droplet. Similar to the results in Fig. 1, confinement increases the initial droplet deformation and slows down the droplet retraction. However, from a comparison between Figs. 1 and 3 it can be seen that, when the matrix is viscoelastic, the initial droplet deformation is less than that of a droplet in a Newtonian matrix, a trend that is well-known (Maffettone and Greco 2004; Minale 2004; Verhulst et al. 2007, 2009a; Cardinaels et al. 2009). The confined Minale model for systems with viscoelastic components predicts a slower droplet retraction when the matrix is viscoelastic as compared to the case with a Newtonian matrix. However, in the experimental data, the effect of matrix viscoelasticity is moderate in bulk conditions and completely absent in confined conditions.

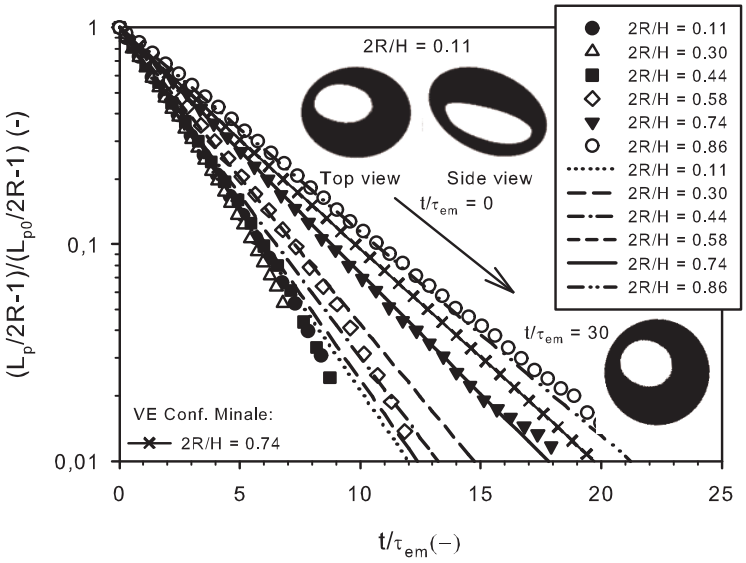

Fig. 2 Droplet retraction after cessation of shear flow with Ca = 0.2 for a series of confinement ratios; Viscoelastic droplet in a Newtonian matrix with λ = 1.5, experimental data (symbols) and predictions of the confined Minale models for systems with Newtonian components (Minale 2008) (lines) or systems with a viscoelastic droplet (Minale et al. 2010) (line with crosses)

To systematically study the effects of confinement and component viscoelasticity on droplet relaxation, data have also been gathered with the system of Fig. 3 for a series of confinement ratios. In addition, experiments have been performed for systems with λ = 0.45, containing either a viscoelastic matrix or a viscoelastic droplet (Blends 3 and 4 in Table 1). Finally, whereas all the previously mentioned data were gathered at a De-number of 1, additional data have been obtained on a system with a viscoelastic droplet and a higher De-number. To provide a comprehensive overview of the effects of the different parameters on the relaxation process, the droplet relaxation times τ for all systems and experimental conditions were determined from plots similar to those in Fig. 2. It should be noted however that for the systems with a viscoelastic matrix, the relaxation becomes slower in the later stages of the

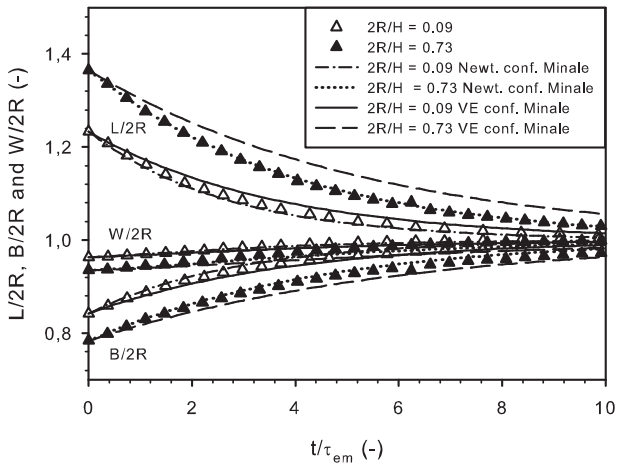

Fig. 3 Dimensionless droplet axes during shape relaxation after cessation of shear flow with Ca = 0.2; Newtonian droplet in a viscoelastic matrix with λ = 1.5, experimental data (symbols) and predictions of the confined Minale models (Minale 2008; Minale et al. 2010) (lines)

relaxation process, resulting in a tail in the relaxation curves, as in Sibillo et al. (2006) and Verhulst et al. (2007, 2009b). However, the latter occurs at very low values of the droplet deformation. Therefore, a substantial linear part is present in the relaxation curves, from which τ can be determined without difficulty. The relaxation times are made dimensionless with the respective emulsion times to eliminate the effect of different matrix viscosities. The results are summarized in Fig. 4, where the dimensionless relaxation times are plotted as a function of the confinement ratio 2R/H.

The bulk results in Fig. 4 show that viscoelasticity of the matrix fluid slightly retards the droplet relaxation at both viscosity ratios. This effect is already clearly established in literature, both experimentally and numerically (Yue et al. 2005; Sibillo et al. 2006; Verhulst et al. 2007, 2009b). Results for droplet relaxation in systems with a viscoelastic droplet

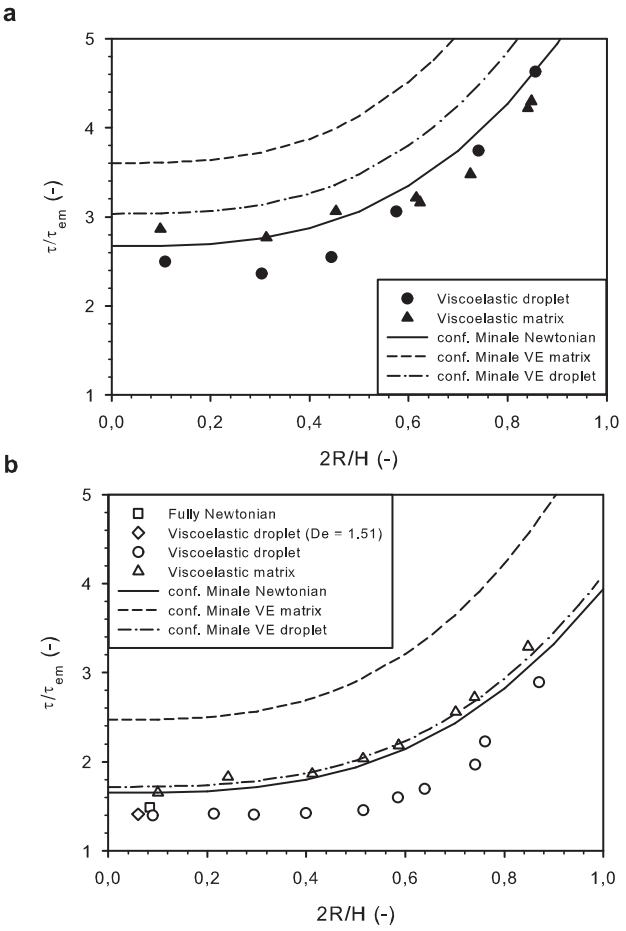

Fig. 4 Dimensionless relaxation time as a function of confinement ratio for ellipsoidal droplets, as determined from droplet retraction after cessation of shear flow with Ca = 0.2, experimental data (symbols) and predictions of the confined Minale models (Minale 2008; Minale et al. 2010) (lines); **a** λ = 1.5, **b** λ = 0.45

are however scarce in literature. Verhulst et al. (2009b) showed that at a viscosity ratio of 1.5, droplet viscoelasticity has no influence on the relaxation process in bulk conditions. At a viscosity ratio of 1, Lerdwijitjarud et al. (2003) did not observe any effect of droplet viscoelasticity either. However, in the latter work the De-number was restricted to values well below 0.5. From the results in Fig. 4b it becomes obvious that, also for lower viscosity

ratios, droplet viscoelasticity has no influence on the relaxation process, and this up to De-numbers above 1.

For all the systems investigated, the threshold value above which confinement effects come into play is comparable and equals approximately 0.5, independent of the component elasticity and the viscosity ratio. For confined droplets, the relaxation process is hampered by the fact that the matrix fluid has to be squeezed out between the plates and the droplet (Janssen and Anderson 2007). The overall relaxation for the systems with $\lambda = 0.45$ is approximately 1.7 times faster than for the systems with viscosity ratio 1.5. Still, confinement effects on the relaxation time are similar for both viscosity ratios, indicating that, within the range of studied material parameters and experimental conditions, a faster retraction does not amplify the hindrance of the relaxation due to the presence of the walls. Upon detailed inspection of the data in Fig. 4 it can be observed that at $\lambda = 0.45$ relaxation in a viscoelastic matrix is always slower than when the droplet is viscoelastic. However, at a viscosity ratio of 1.5, the trend reverses and the relaxation of viscoelastic droplets becomes slightly slower than that of Newtonian droplets in a viscoelastic matrix. Cardinaels et al. (2009) have shown that for systems with a viscosity ratio of 1.5, droplets in a viscoelastic matrix are less deformed than those in a Newtonian matrix at all confinement ratios, whereas for systems with a viscosity ratio of 0.45, droplet deformation becomes nearly independent of the fluid viscoelasticity at the highest confinement ratios. In addition, at a viscosity ratio of 1.5, matrix viscoelasticity postpones the transition from ellipsoidal to sigmoidal droplet shapes to higher Ca-numbers and confinement ratios as compared to a Newtonian matrix (Cardinaels et al. 2009). Therefore, the slightly faster relaxation for a viscoelastic matrix as compared to a viscoelastic droplet at a viscosity ratio of 1.5 and high confinement ratios might be caused by differences in the initial deformation or shape of the droplets.

The dimensionless relaxation times τ_{conf} obtained from the confined Minale models for systems with Newtonian (Minale 2008) and viscoelastic components (Minale et al. 2010) are also included in Fig. 4. These are calculated according to:

$$\frac{\tau_{conf}}{\tau_{em}} = \frac{\tau_{bulk}}{\tau_{em}} \cdot \left[1 + C_s (R/H)^3 \cdot \frac{44 + 64\lambda - 13\lambda^2}{2(1+\lambda)(12+\lambda)}\right] \tag{3}$$

where C_s is a parameter that equals 5.7 for a droplet that is situated in the middle of the gap (Shapira and Haber 1990), τ_{bulk} is the relaxation time for the shape relaxation of unbounded ellipsoidal droplets (Mo et al. 2000):

$$\frac{\tau_{bulk}}{\tau_{em}} = \frac{1}{f_1} \tag{4}$$

and f_1 is a parameter in the bulk Maffettone-Minale (Maffettone and Minale 1998) and Minale models (Minale 2004). It can be deduced from Eq. 3 that both confined Minale models predict a relaxation time that is independent of the initial droplet deformation and gradually increases with R/H to the power 3. Theoretically, the phenomenological models only predict an exponential decay for the relaxation of the differences of the squared semiaxes of the droplet, such as L^2-B^2, with L and B the longest and shortest droplet axis in the velocity-velocity gradient plane (Mo et al. 2000). However, it is shown in Fig. 2 that for the scaled projection L_p of the longest axis L in the velocity direction, the deviations from an exponential relaxation are insignificant. In addition, it has carefully been checked that the predicted droplet relaxation times obtained from curves as in Fig. 2 agree with those obtained from Eqs. 3 and 4. Therefore, the latter equations are plotted in Fig. 4.

Figure 4 shows that the predictions of the confined Minale models qualitatively capture the trends as a function of confinement ratio, although wall effects start well below 2R/H

= 0.5, which is not in agreement with the experimental results. A similar conclusion was reported by Vananroye et al. (2008) for blends that contain only Newtonian components. For both viscosity ratios, the model predicts a significant retardation of the relaxation when the matrix is viscoelastic. This is in qualitative agreement with the data, but the predicted effect is more pronounced than the experimentally observed one. A preliminary validation of the confined Minale model for systems with viscoelastic components has already been performed for droplet relaxation in a viscoelastic matrix at 2R/H = 0.74 (Minale et al. 2010). Although they studied an initially highly deformed droplet and the amount of data during the exponential part of the relaxation curve is limited, the results suggest a good agreement between the model predictions and the experimental data at De = 1.1. This conclusion is not supported by the results presented in Fig. 4. The confined Minale model for systems with viscoelastic components has been derived for blends that consist of second-order fluids (Minale et al. 2010). Despite the fact that in the range of shear rates that is relevant in the present study the steady shear rheology of the used Boger fluid can be well described by means of the second-order fluids model, Boger fluids have a spectrum of relaxation times that can affect the kinetics of shape relaxation (Verhulst et al. 2009b). The Boger fluid in the work of Minale et al. (2010) contains a higher percentage of high molecular weight component and the latter has a lower molecular weight as compared to the polymer used in the present work. Hence, the spectrum of relaxation times of the fluids in both works and their elongational viscosity is expected to be different and this might cause differences in the droplet behaviour. Therefore, it can be concluded that, despite the qualitative agreement, even at the same De, the kinetics of shape relaxation can vary, depending on the details of the viscoelastic fluid. These effects are however not included in the second-order fluids model, which can lead to deviations between the experimental data and the model predictions.

For systems with a viscoelastic droplet in confinement, no model predictions or experimental data are available in literature. Fig. 4 shows that the effects of droplet viscoelasticity on the model predictions are less pronounced as the effects of matrix viscoelasticity, especially at a viscosity ratio of 0.45. Experimentally, no effect of droplet viscoelasticity was observed. Finally, the model predictions form parallel lines as a function of confinement ratio, indicating that confinement and viscoelasticity effects are completely decoupled. However, the experimental data show a more complex picture, in which the effects of component viscoelasticity on the droplet relaxation time depend on the confinement ratio. Finally, it should be noted that the presentation method of Figs. 2 and 4 is a more straightforward and sensitive way to differentiate between the different relaxation curves as compared to a plot of the droplet axes.

4.2 Shape relaxation after shear flow at a Ca close to the critical conditions

In this section, the retraction of droplets at a Ca-number that is close to the critical value Ca_{crit} will be discussed. The values of the applied Ca-number are Ca = 0.35 for systems with a viscosity ratio of 1.5 ($Ca_{crit,bulk}$ = 0.56) and Ca = 0.4 for systems with a viscosity ratio of 0.45 ($Ca_{crit,bulk}$ = 0.46). The apparent different distance from the critical conditions is motivated by the different trend of the critical Ca-number as a function of confinement ratio for systems with viscosity ratios above and below one. For viscosity ratios above 1 and systems that contain only Newtonian components, the critical Ca-number for breakup decreases with increasing confinement. The opposite trend was observed for systems with a viscosity ratio below 1 (Vananroye et al. 2006). Therefore, a lower Ca-number is used here for the system with the highest viscosity ratio as compared to the system with the lower viscosity ratio.

Experimental results for shape relaxation in systems with a viscosity ratio of 1.5 are shown in Fig. 5a and 5b for respectively a viscoelastic droplet and a viscoelastic matrix. At a Ca-number of 0.35, the initial droplet shape for the highly confined droplets is no longer ellipsoidal, but sigmoidal, as shown in the insert of Fig. 5a. The sigmoidal droplet shape causes the relaxation of the longest axis L to be initially slow, resulting in a shoulder in the relaxation curves. Subsequently, the droplet attains a dumbbell-like shape before becoming an ellipsoid. This type of relaxation, consisting of an initial relaxation by means of a shape change without significant reduction of the droplet length, followed by a simple droplet retraction, was reported on by several authors (Stone et al. (1986); Yamane et al. (1998); Hayashi et al. (2001a); Assighaou and Benyahia (2008); Renardy et al. (2009)). In those studies, the highly deformed non-ellipsoidal droplet shape was however generated by applying flow with a supercritical Ca rather than confining the droplet between parallel plates. Nevertheless, the qualitative nature of the relaxation process of non-ellipsoidal droplets seems to be rather universal. Curves with a slope that is calculated from the relaxation times in Fig. 4 are added as full lines in Fig. 5a. It can be concluded that the experimental relaxation times for the exponential part of the relaxation process agree very well with the relaxation times obtained from the relaxation of initially ellipsoidal droplets (from Fig. 4).

When comparing the results of Fig. 5a for a viscoelastic droplet with those of Fig. 5b for a viscoelastic matrix, it is clear that the shoulder is less pronounced for the systems with a viscoelastic matrix. This is in agreement with the difference in steady state droplet shapes reported in Cardinaels et al. (2009): at a viscosity ratio of 1.5 and the same Ca, a droplet is less deformed in a viscoelastic matrix as compared to a Newtonian matrix and also shows less tendency to be sigmoidal. The phenomenological models, that were developed for ellip-

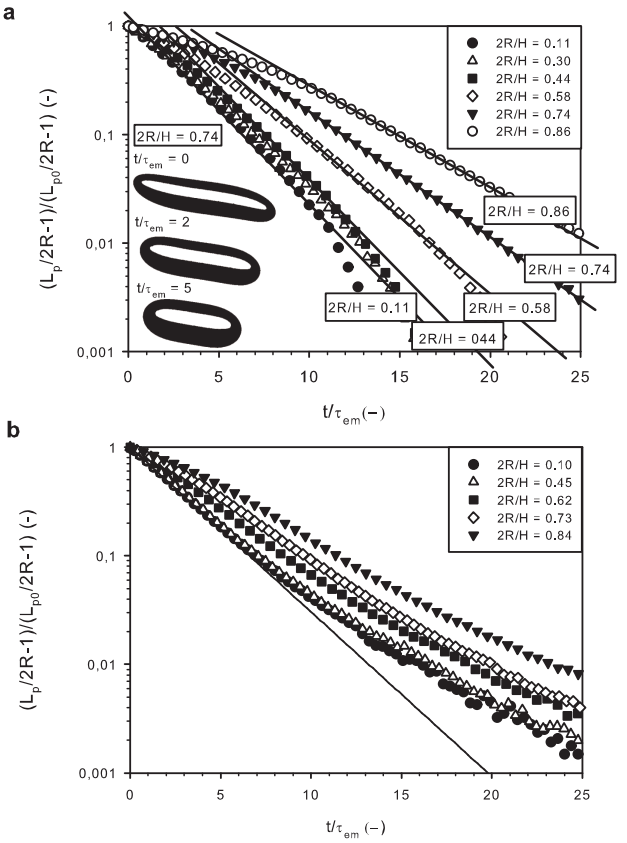

Fig. 5 Droplet retraction after cessation of shear flow close to the critical conditions for a series of confinement ratios (Ca = 0.35 and λ = 1.5); **a** Viscoelastic droplet, lines have a slope calculated from the relaxation times in Fig. 4, insert: droplet shapes obtained in the velocity - velocity gradient plane during retraction of a highly confined droplet, **b** Viscoelastic matrix, the line represents the initial exponential relaxation of an unconfined droplet

soidal droplets, predict a too fast initial retraction for the sigmoidal droplets, similar to the case of non-ellipsoidal droplets obtained after a step-strain (Jackson and Tucker 2003; Yu and Bousmina 2003). Therefore, model predictions are omitted in this section. The line in Fig. 5b represents an exponential relaxation with a relaxation time for an unbounded droplet in a viscoelastic matrix at viscosity ratio λ = 1.5, as obtained from Fig. 4. The experimen-

tal curves in Fig. 5b show that the droplet retraction at the end of the relaxation process is slowed down as compared to an exponential relaxation, leading to a tail in the relaxation curves, as in Sibillo et al. (2006) and Verhulst et al. (2007, 2009b) for bulk conditions. Verhulst et al. (2009b) have shown that this deviation from an exponential relaxation is caused by the multiple relaxation times of the Boger fluid matrix. It should be remarked here that Minale et al. (2010) reported a relaxation with a single relaxation time for a confined droplet in a viscoelastic matrix at De = 1.1 and 2R/H = 0.74. However, as discussed before, the molecular weight of the polymer in the Boger fluid matrix was substantially lower in their work as compared to the present work, which most probably results in a Boger fluid with less contributions from very long relaxation times. The absence of long relaxation times in the Boger fluid rheology can cause the absence of a tail in the shape relaxation curves of Minale et al. (2010).

Similar to Fig. 5, the droplet dynamics after cessation of shear flow in systems with a lower viscosity ratio (λ = 0.45) are shown in Fig. 6. In this case, the Ca-number of the preceding shear flow is 0.4. The results are qualitatively similar to those shown in Fig. 5. The shoulder is however less clear, which can be attributed to the fact that confinement effects on the steady state deformation are less pronounced at this lower viscosity ratio (Vananroye et al. 2007; Cardinaels et al. 2009). Hence, the droplet shape remains ellipsoidal up to high confinement ratios. The relaxation times for the viscoelastic droplet, obtained from the linear part of the relaxation curves, again agree well with the results obtained for an ellipsoidal droplet that relaxes after a steady shear flow with Ca = 0.2. This is illustrated in Fig. 6a for the highest confinement ratio (2R/H = 0.83), where a line with a slope that is calculated from the relaxation time at this confinement ratio, as obtained from Fig. 4, is superimposed on the experimental data.

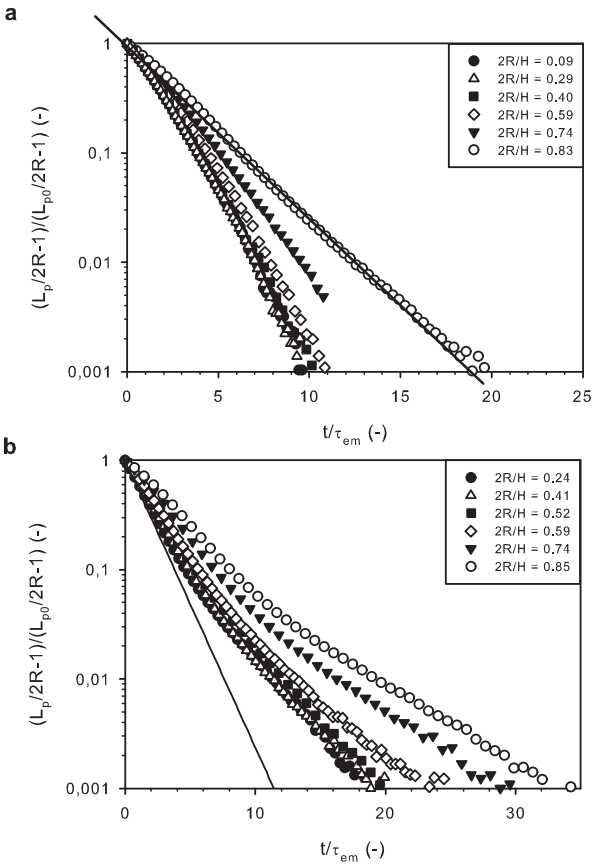

Fig. 6 Droplet retraction after cessation of shear flow close to the critical conditions for a series of confinement ratios (Ca = 0.4 and λ = 0.45); **a** Viscoelastic droplet, line has a slope calculated from the relaxation time in Fig. 4, **b** Viscoelastic matrix, the line represents the initial exponential relaxation of an unconfined droplet

The line in Fig. 6b for a system with a viscoelastic matrix depicts an exponential relaxation, for which the relaxation time is obtained from Fig. 4 for bulk conditions. Also at this viscosity ratio, as in Fig. 5b, matrix viscoelasticity clearly causes a tail in the relaxation curves. From a comparison of simulated relaxation curves obtained with and without incorporating an initial stress field, Yue et al. (2005) have shown that this tail is the combined result of

the relaxing viscoelastic stresses that constrain the droplet retraction and the stretching of the polymer chains at the droplet tips due to the retraction process. The longest relaxation time of the Boger fluid matrix material that is used here, expressed in the dimensionless time units of Figs. 5 and 6 is approximately 18 and the relaxing viscoelastic stresses might thus influence the relaxation process. When comparing the results of Fig. 5b at a viscosity ratio of 1.5 with those of Fig. 6b at a viscosity ratio of 0.45, it can be seen that the tail is more pronounced for the system with the lowest viscosity ratio, although both systems have an almost identical emulsion time and polymer relaxation time (= same De). At λ = 0.45, the droplet relaxation is about twice as fast as at λ = 1.5, which increases the ratio of polymer relaxation time to droplet relaxation time. This clearly amplifies the effect of viscoelasticity on the droplet retraction. The transition point between the linear part of the relaxation curve and the tail can be estimated from the intersection of the initial and final linear parts of the curves. Fig. 6b shows that the transition occurs for a value of the dimensionless Lp-axis of around 0.04, while the dimensionless time of the transition varies between 8 and 13. Hence, the transition point seems to be more related to the amount of droplet relaxation rather than to the time. Therefore, these experiments indicate that there might be an interaction between the polymer relaxation and the retracting droplet, which further elongates the polymer molecules or at least postpones their recoil. The latter is in agreement with the mechanism proposed by Yue et al. (2005). It should be noted however that the effect of confinement on the relaxation kinetics of the viscoelastic stresses is unknown at present.

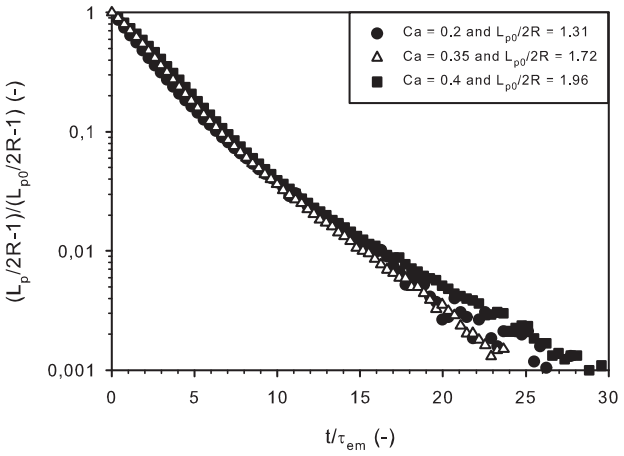

Fig. 7 Droplet retraction after cessation of shear flow for a Newtonian droplet in a viscoelastic matrix with λ = 0.45, 2R/H = 0.74 and different Ca-numbers

4.3 Master curves for shape relaxation

Finally, the effect of the initial droplet deformation on the shape relaxation kinetics is illustrated in Fig. 7. This figure shows relaxation curves for a confined Newtonian droplet in a viscoelastic matrix (2R/H = 0.74 and λ = 0.45) after cessation of shear flow with different Ca. For the conditions shown in Fig. 7, the curves of the scaled projected axis L_p form a master curve for different initial droplet elongation ratios $L_{p0}/2R$. At high confinement ratios and Ca-numbers, the most deformed droplets have a sigmoidal shape and a shoulder appears in the retraction curves, which limits the existence of master curves to ellipsoidal droplet shapes. At a viscosity ratio of 1.5 (see Fig. 5), this restricts superposition to lower confinement ratios.

5 Conclusions

The effects of geometrical confinement and component viscoelasticity on shape relaxation after cessation of shear flow are studied microscopically for single droplets. As viscoelastic component, a model Boger fluid is used, which is rheologically fully characterized, both in shear and extensional flow (Verhulst et al. 2007, 2009a,b). This makes the presented data sets suitable as a reference for future modelling.

Deformed droplets are generated by applying a shear flow with a subcritical flow intensity. Viscoelasticity of the droplet fluid does not have any measurable influence on the relaxation process, whereas geometrical confinement and matrix viscoelasticity both retard the shape relaxation of deformed droplets. Although confined droplets relax considerably slower than unconfined ones, allowing more time for the polymeric viscoelastic stresses to relax, the well-known tail in the relaxation curves (Sibillo et al. 2006; Verhulst et al. 2007, 2009b) remains present for droplets in a viscoelastic Boger fluid matrix. As long as the initial droplet shape is ellipsoidal, the relaxation kinetics is independent of the initial deformation and master curves can be constructed. However, confined droplets can become sigmoidal, and this causes a slowing down of the initial stage of the relaxation process.

The experimental data for ellipsoidal droplets have been compared to the predictions of two phenomenological models for droplet dynamics in confined systems with either only Newtonian components or with one viscoelastic component (Minale 2008; Minale et al. 2010). The effect of geometrical confinement is qualitatively captured by the model. However, whereas the model assumes a complete decoupling of viscoelasticity and confinement effects, the experimental data clearly show that the behaviour is more complex. Finally, by

comparing the results obtained in this work with the results of Minale et al. (2010), it can be concluded that, even at the same Deborah number, small differences in the Boger fluid rheology can influence the droplet relaxation behaviour.

Acknowledgements R. Cardinaels is indebted to the Research Foundation - Flanders (FWO) for a Ph. D. Fellowship. This work is partially funded by Onderzoeksfonds K.U.Leuven (GOA09/002).

References

Assighaou S, Benyahia L (2008) Universal retraction process of a droplet shape after a large strain jump. Phys Rev E 77:036305/1-5

Briscoe BJ, Lawrence CJ, Mietus WGP (1999) A review of immiscible fluid mixing. Adv Colloid Int Sci 81:1-17

Cardinaels R, Verhulst K, Moldenaers P (2007) Drop shape dynamics during shear flow in blends with a viscoelastic component: Bulk and confined conditions. In: Proc 9th European Symposium on Polymer Blends, Palermo (Italy), 8 pages on CD-rom

Cardinaels R, Verhulst K, Renardy Y, Moldenaers P (2008) Transient droplet behavior and droplet breakup during bulk and confined shear flow in blends with one viscoelastic component: Experiments, modelling and simulations. In: Co A, Leal LG, Colby RH, Giacomin AJ Proc The XVth International Congress on Rheology, Monterey (USA), pp 1405-1407

Cardinaels R, Verhulst K, Moldenaers P (2009) Influence of confinement on the steady state behaviour of single droplets in shear flow for immiscible blends with one viscoelastic component. J Rheol 53:1403-1424

De Bruijn RA (1989) Deformation and breakup of droplets in simple shear flows. PhD Thesis, Eindhoven University of Technology

Fenouillot F, Cassagnau P, Majest*é* JC (2009) Uneven distribution of nanoparticles in immiscible fluids: Morphology development in polymer blends. Polymer 50:1333-1350

Grace HP (1982) Immiscible fluid systems and application of static mixers as dispersion devices in such systems. Chem Eng Commun 14:225-277

Greco F (2002) Drop deformation for non-Newtonian fluids in slow flows. J Non-Newton Fluid Mech 107:111-131

Guido S, Villone M (1999) Measurement of interfacial tension by drop retraction analysis. J Colloid Int Sci 209:247-250

Guido S, Greco F (2001) Drop shape under slow steady shear flow and during relaxation. Experimental results and comparison with theory. Rheol Acta 40:176-184

Guido S, Greco F (2004) Dynamics of a liquid drop in a flowing immiscible liquid. In: Binding DM and Walters K Rheology Reviews, The British Society of Rheology, Aberystwyth, pp 99-142

Hayashi R, Takahashi M, Yamane H, Jinnai H, Watanabe H (2001) Dynamic interfacial properties of polymer blends under large step strains: shape recovery of a single droplet. Polymer 42:757-764

Jackson NE, Tucker CL (2003) A model for large deformation of an ellipsoidal droplet with interfacial tension. J Rheol 47:659-682

Janssen PJA, Anderson PD (2007) Boundary-integral method for drop deformation between parallel plates. Phys Fluids 19:043602/1-11

Lerdwijitjarud W, Larson RG, Sirivat A, Solomon MJ (2003) Influence of weak elasticity of dispersed phase on droplet behavior in sheared polybutadiene/poly(dimethylsiloxane) blends. J Rheol 47:37-58

Luciani A, Champagne MF, Utracki LA (1997) Interfacial tension coefficient from the retraction of ellipsoidal drops. J Polym Sci Part B 35:1393-1403

Maffettone PL, Minale M (1998) Equation of change for ellipsoidal drops in viscous flow. J Non-Newton Fluid Mech 78:227-241; Erratum: J Non-Newton Fluid Mech 84:105-106

Maffettone PL, Greco F (2004) Ellipsoidal drop model for single droplet dynamics with non-Newtonian fluids. J Rheol 48:83-100

Minale M (2004) Deformation of a non-Newtonian ellipsoidal drop in a non-Newtonian matrix: extension of Maffettone-Minale model. J Non-Newton Fluid Mech 123:151-160

Minale M (2008) A phenomenological model for wall effects on the deformation of an ellipsoidal drop in viscous flow. Rheol Acta 47:667-675

Minale M, Caserta S, Guido S (2010) Microconfined shear deformation of a droplet in an equiviscous non-newtonian immiscible fluid: Experiments and modelling. Langmuir 26:126-132

Mo H, Zhou C, Yu W (2000) A new method to determine interfacial tension from the retraction of ellipsoidal droplets. J Non-Newton Fluid Mech 91:221-232

Quinzani LM, McKinley GH, Brown RA, Armstrong RC (1990) Modeling the rheology of polyisobutylene solutions. J Rheol 34:705-748

Rallison JM (1984) The deformation of small viscous drops and bubbles in shear flows. Annu Rev Fluid Mech 16:45-66

Renardy Y, Renardy M, Assighaou S, Benyahia L (2009) Numerical simulation of drop retraction after a strain jump. Phys Rev E 79:046323/1-4

Shapira M, Haber S (1990) Low Reynolds number motion of a droplet in shear flow including wall effects. Int J Multiphase Flow 16:305-321

Sibillo V, Simeone M, Guido S, Greco F, Maffettone PL (2006) Start-up and retraction dynamics of a Newtonian drop in a viscoelastic matrix under simple shear flow. J Non-Newton Fluid Mech 134:27-32

Stone HA, Bentley BJ, Leal LG (1986) An experimental study of transient effects in the breakup of viscous drops. J Fluid Mech 173:131-158

Stone HA (1994) Dynamics of drop deformation and breakup in viscous fluids. Annu Rev Fluid Mech 26:65-102.

Taylor GI (1932) The viscosity of a fluid containing small drops of another fluid. Proc R Soc London A 138:41-48

Taylor GI (1934) The formation of emulsions in definable fields of flow. Proc R Soc London A 146:501-523

Tucker III CL, Moldenaers P (2002) Microstructural evolution in polymer blends. Annu Rev Fluid Mech 34:177-210

Vananroye A, Van Puyvelde P, Moldenaers P (2006) Effect of confinement on droplet breakup in sheared emulsions. Langmuir 22:3972-3974

Vananroye A, Van Puyvelde P, Moldenaers P (2007) Effect of confinement on the steady-state of single droplets during shear flow. J Rheol 51:139-153

Vananroye A, Cardinaels R, Van Puyvelde P, Moldenaers P (2008) Effect of confinement and viscosity ratio on the dynamics of single droplets during transient shear flow. J Rheol 52:1459-1475

Van Puyvelde P, Moldenaers P (2005) Rheology and morphology development in immiscible polymer blends. In: Binding DM and Walters K Rheology Reviews, The British Society of Rheology, Aberystwyth, pp 101-145

Van Puyvelde P, Vananroye A, Cardinaels R, Moldenaers P (2008) Review on morphology development of immiscible blends in confined shear flow. Polymer 49:5363-5372

Verhulst K, Moldenaers P, Minale M (2007) Drope shape dynamics of a Newtonian drop in a non-Newtonian matrix during transient and steady shear flow. J Rheol 51:261-273

Verhulst K, Cardinaels R, Moldenaers P, Renardy Y, Afkhami S (2009a) Influence of viscoelasticity on drop deformation and orientation in shear flow: Part 1. Stationary states. J Non-Newton Fluid Mech 156:29-43

Verhulst K, Cardinaels R, Moldenaers P, Afkhami S, Renardy Y (2009b) Influence of viscoelasticity on drop deformation and orientation in shear flow. Part 2: Dynamics. J Non-Newton Fluid Mech 156:44-57

Yamane H, Takahashi M, Hayashi R, Okamoto K, Kashihara H, Masuda T (1998) Observation of deformation and recovery of poly(isobutylene) droplet in a poly(isobutylene)/poly(dimethyl siloxane) blend after application of step shear strain. J Rheol 42:567-580

Yu W, Bousmina M (2003) Ellipsoidal model for droplet deformation in emulsions. J Rheol 47:1011-1039

Yu W, Bousmina M, Zhou C, Tucker III CL (2004) Theory for drop deformation in viscoelastic systems. J Rheol 48:417-438

Yu W, Zhou C, Bousmina M (2005) Theory of morphology evolution in mixtures of viscoelastic immiscible components. J Rheol 49:215-236

Yue P, Feng JJ, Liu C, Shen J (2005) Diffuse-interface simulations of drop coalescence and retraction in viscoelastic fluids. J Non-Newton Fluid Mech 129:163-176